An in Situ Scanning Tunneling Microscopy and Cyclic Voltammetric Study of Iodobenzene and Iodoheptane Molecules Adsorbed on a Pt(111) Electrode†

Jung-Huein Chen,‡ Shueh-Lin Yau,*,‡ and Si-Chung Chang§

Department of Chemistry, National Central University, ChungLi, Taiwan 320, Republic of China, and Helix Cooperation, Hsinchu, Taiwan 300, Republic of China

Received: January 24, 2002; In Final Form: April 15, 2002

We employed in situ scanning tunneling microscopy (STM) and cyclic voltammetry to study the adsorption of iodobenzene and iodoheptane molecules onto a well-ordered Pt(111) electrode in 0.1 M $HClO_4$. These molecules were adsorbed intact without noticeable decomposition at potentials negative of 0.9 V (vs a reversible hydrogen electrode), whereas degradation became prominent at potentials positive of 0.9 V. The coverage of the iodobenzene monolayer is estimated to be about 0.45 from the amount of charges involved in its reductive desorption in $KClO_4$ (pH 10) solutions. This value nearly equals that of iodine atoms at Pt(111). In situ STM was used to probe the spatial arrangements of these adsorbates as a function of potential in 0.1 M $HClO_4$. A well-packed $(\sqrt{7} \times \sqrt{7})R19.1°$−iodobenzene structure predominated at 0.3 V, which readily rearranged into a (3×3) adlattice as a result of a slight increase of coverage at more positive potentials. The STM appearances of these two adlattices resemble those of iodine atoms on Pt(111), suggesting that the contrast in STM arises mainly from the iodine headgroups. More negative potentials resulted in desorption of iodobenzene molecules and a disordered adlayer. In contrast, iodoheptane molecules were disordered at potentials negative of 0.7 V, but reorganization occurred to produce local $(\sqrt{7} \times \sqrt{7})R19.1°$ at more positive potentials. These phase transitions were reversible to the modulation of potential between 0 and 0.9 V. The electrochemical potential dominated not only the chemical nature but also the spatial arrangements of the alkyl or aryl iodide molecules. The tip-and-sample interaction was noticeably stronger for iodoheptane, resulting in disordering of the adlayer.

Introduction

Scanning tunneling microscopy (STM), invented in the early 1980s,[1] finds extensive applications in probing surface structures in ultrahigh vacuum (UHV), ambient conditions, and electrolyte solutions.[2] STM can provide atomic or molecular resolution of adsorbates, residing on metallic and semiconducting substrates. While subnanometer resolution has been ubiquitous for STM, the origin of contrast in the atomic or molecular resolution of STM can be elusive. Thanks to the advances of theoretical and experimental endeavor in recent years, the imaging mechanism of STM becomes much more tractable now, at least for the STM results obtained in UHV. This progress greatly helps the interpretation of STM results. The electron tunneling event can be considered as the sum of two components, through-surface and through-adsorbate.[3,4] These two components frequently counteract on the STM imaging process, and the superior factor eventually determines the appearances of atomic or molecular adsorbates.[3] These models successfully explain the relative corrugation heights of B, C, N, O, S, and Al atoms on metallic substrates.[3] The atomic-orbital exponents, which determine the extensions in the space of orbitals, are found to govern the appearances of adsorbates in the STM images.[3] These theoretical models pave the way for the identification of adatoms (C, N, O, F, and S) on Pd(111) surfaces.[4]

As for molecular adsorbates, the electron tunneling event occurring between the tip of the scanning tunneling microscope and a sample becomes complex. Depending on the chemical structures of adsorbates, different tunneling mechanisms are devised to account for the outcome of STM measurements. Not only the electronic structures but also the spatial arrangements of molecular orbitals of an adsorbate can influence the topography of STM images. For example, a detailed study of the molecular orbitals of benzene molecules chemisorbed at various sites on a Pt(111) surface results in a tangible model for the STM molecular resolution.[5] Typically, aromatic molecules of benzene, naphthalene, and others are adsorbed with their molecular planes parallel to the surface, rendering specifically shaped molecular features.[6] Furthermore, STM imaging is shown to reflect the electron density contours of the highest occupied molecular orbitals (HOMOs) of the para-substituted phenyl octadecyl ethers adsorbed on highly oriented pyrolytic graphite (HOPG).[7] With its tip coated with 4-mercaptopyridine, the scanning tunneling microscope discriminates the presence of Zn^{2+} ions coordinated at the centers of porphyrin.[8] Consequently, the chemical interactions between the tip and adsorbates through hydrogen bonding and metal−ligand coordinations can influence the outcome of STM measurements.[6−8]

On the other hand, to comprehend the STM results for molecular adsorbates arranged vertically on a substrate, a mechanism based on lowering of the tunneling barrier was established to explain, for example, the well-known self-assembled alkanethiol monolayers on Au(111).[8] Specifically, the effect of the sulfur headgroup in lowering substantially the local work function by more than 1 eV apparently dominates

* To whom correspondence should be addressed. E-mail:philyau@cc.ncu.edu.tw. Phone: 886-3-4227151-5909. Fax: 886-3-4227664.

† This paper is dedicated to Prof. Michael J. Weaver, in memory of his great contribution to the study of interfacial electrochemistry.

‡ National Central University.

§ Helix Cooperation.

10.1021/jp020236k CCC: $22.00
Published on Web 08/09/2002

the electron tunneling process. The aliphatic hydrocarbon chains of alkanethiol molecules do not contribute to electron tunneling. Furthermore, recent studies in UHV indicate that it is necessary to use an ultralow tunneling current of 1−10 pA at a bias voltage of 10−1000 mV to facilitate molecular resolution with minimal perturbation to the adlayers.[9−13] This high-gap-impedance STM is further advantageous in discriminating different functional groups, such as −OH and $-CH_3$, at the ends of alkanethiol molecules adsorbed on Au.[13] Nevertheless, rather different parameters, such as 0.5−2 nA and 500−1000 mV, could result in molecular resolutions of alkanethiol molecules in ambient conditions and in solutions.[14−17]

Here we employ in situ STM and cyclic voltammetry (CV) to examine the adsorption of iodobenzene and iodoheptane molecules on a well-defined Pt(111) electrode. We address (1) the prominent role of electrochemical potential in governing the surface bonding, (2) the imaging mechanism of in situ STM, and (3) the real-space structures of these molecules as compared to those of iodine atoms. The choice of iodine as the headgroup of the molecular adsorbates is due to the fact that the adsorption of iodine atoms at Pt(111) is characterized by STM and UHV tools.[18−20] Our STM and CV results show that the iodo molecules are adsorbed intact without decomposition within a certain potential range. This is in strong contrast to the previous UHV results showing extensive decompositions of alkyl and aryl iodides on Au, Pt, Pd, Ag, and Cu in UHV at room temperature.[21−25] This disparity highlights the critical roles of interfacial environments in determining the adsorption process and the subsequent chemical or electrochemical reactions. Furthermore, iodobenzene molecules were adsorbed in well-ordered (3 × 3) and ($\sqrt{7} \times \sqrt{7}$)*R*19.1°, previously identified for iodine atoms on Pt(111).[20] In contrast, alkyl iodides such as iodoheptane and iodododecane only formed local ($\sqrt{7} \times \sqrt{7}$)-*R*19.1°. The degree of ordering of the molecular monolayer might affect the quality of STM imaging. We noted strong tip-and-sample interaction when imaging iodoheptane, rendering significant instability to the STM experiments. We could achieve high-quality STM molecular images with 5 nA and 200 mV, which are very different from those used for imaging alkanethiol in UHV.[11−13]

Experimental Section

Pretreatment of the Pt(111) Electrode. Preparation of single-crystal bead electrodes of platinum followed Clavilier's procedure described elsewhere.[26] Electrode pretreatment involved annealing with a hydrogen torch, cooling in a H_2 and N_2 mixed stream, and quenching in hydrogen-saturated Millipore water (resistivity >18.2 MΩ). The electrodes were then quickly transferred into the electrochemical or STM cell under protection of a thin water film. Due to the presence of an oxide layer on the *as-prepared* Pt, their open-circuit potentials were normally near 0.9 V. The potential was usually swept negatively to 0.05 V to reduce the oxide layer before the organic compounds of interest were added directly into the STM cell. With its submonolayer sensitivity, cyclic voltammetry is suitable to diagnose the surface states of the as-prepared electrodes.

Chemicals. Ultrapure perchloric acid and potassium iodide were purchased from Merck Inc. (Darmstadt, Germany). Iodobenzene was obtained from Lancaster (Lancashire, U.K.), and iodoheptane and iodododecane were obtained from Acros Co. (Geel, Belgium). They were used as received without further purification. The impurities in the iodo compounds exerted little effect on the molecular structures at the Pt(111) electrode. Millipore triple-distilled water was used to prepare all the needed solutions. The concentrations of all the organic-containing 0.1 M $HClO_4$ solutions were nearly saturated, and they typically contained 0.1 mM organic materials. This solute density is equivalent to 1 Torr of pressure in the gas phase, a value roughly 6−7 orders of magnitude higher than the typical dosing level in UHV. This drastically different dosing level might be critical to the orientations of molecular adsorbates. We also emphasize the important effects of potential on the adsorptive events and chemical natures of these iodo molecules. The molecular adlayers prepared with or without potential holding led to different CV and STM results.

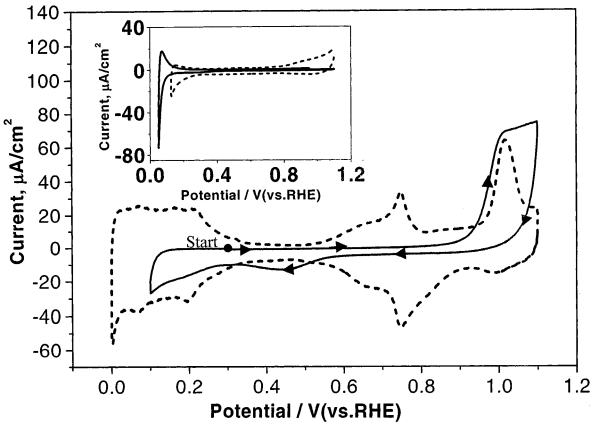

Figure 1. Cyclic voltammograms of Pt(111) at 50 mV/s in 0.1 M $HClO_4$ with (solid trace) and without (dotted trace) the presence of an iodobenzene monolayer. The adsorption of iodobenzene was done under potential control at 0.3 V. The two CV traces in the inset are for Pt(111) electrodes coated with a monolayer of iodine atoms (solid line) or iodobenzene molecules (dotted line) dosed at the open-circuit potential.

In Situ Scanning Tunneling Microscopy. The scanning tunneling microscope was a Nanoscope-E (Santa Barbara, CA), and the tip was made of tungsten (diameter 0.3 mm) prepared by electrochemical etching in 2 M KOH. After thorough rinsing with water and acetone, the tip was further painted with nail polish for insulation. The leakage current of the tip at the open circuit potential was less than 0.05 nA. More than 80% of the as-prepared tips yielded a good resolution. We always used the constant-current mode in the in situ STM imaging experiments. This operation mode was able to give high-quality STM images. Reversible hydrogen electrodes (RHEs) were used in the electrochemical and STM measurements, and all the potentials in the following refer to an RHE scale.

Results and Discussion

Cyclic Voltammetry. The solid and dotted traces in Figure 1 represent, respectively, the cyclic voltammograms at 50 mV/s of iodobenzene (IB)-coated and bare Pt(111) electrodes in 0.1 M $HClO_4$. The dotted trace contains typical hydrogen and oxygen adsorption/desorption features for a well-ordered Pt(111) electrode.[26] With its potential held at 0.3 V, the Pt(111) electrode was made to contact a 0.1 M $HClO_4$ solution containing saturated IB. Five minutes later the electrolyte was drained and replaced with pure 0.1 M $HClO_4$. We then initiated a positive-going potential sweep from 0.3 to 1.1 V at 50 mV/s, resulting in the CV trace shown as a solid line in Figure 1. Double-layer charging prevails between 0.3 and 0.9 V, indicating passivation of the Pt(111) electrode by the adsorption of foreign species, supposedly the iodobenzene molecules. A precipitous increase of the anodic current emerges at 0.9 V but quickly levels off after reaching 1 V. This feature has to arise from irreversible oxidation of the surface-bound IB molecules. According to the UHV results,[21−25] the products might be iodine atoms and some unknown organic fragments, such as phenyl groups. This feature

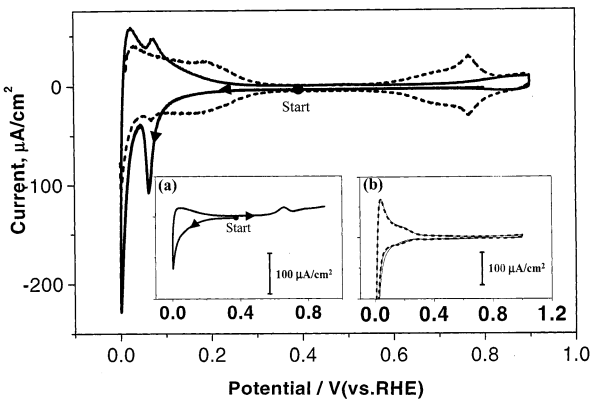

Figure 2. Cyclic voltammograms of Pt(111) at 50 mV/s in 0.1 M $HClO_4$. The solid line represents the 12th cathodic potential sweep after the deposition of an iodobenzene monolayer at 0.4 V. The dotted line was acquired after the potential of Pt(111) was held at 0 V for 10 min. Inset a was obtained for Pt(111) coated with an iodoheptane monolayer. The solid and dotted CV traces in inset b are for iodine-modified Pt-(111) electrodes before and after 10 min of potential holding at 0 V.

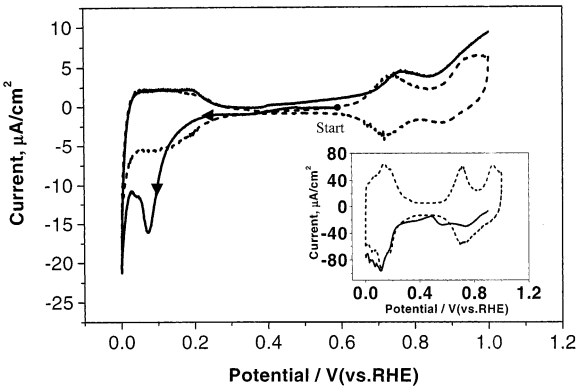

Figure 3. Cyclic voltammograms of Pt(111) at 5 mV/s in pH 10 0.1 M $KClO_4$. The solid line represents the first cathodic potential sweep after the deposition of an iodobenzene monolayer at 0.6 V. Reversing the potential sweep at 0 V resulted in the dotted line. Similar experiments were performed for Pt(111) modified with an iodine adlayer but in pH 13 0.1 M KOH solutions, leading to the solid and dotted CV traces in the inset.

gradually diminishes with continuous potential cycling between 0.1 and 1.1 V (not shown). The details of these anodic processes are however unclear. They are intricate and slow processes, as commonly observed for the oxidation of iodine atoms and aromatic molecules at Pt electrodes.[2]

We also performed similar CV experiments with iodobenzene molecules deposited on Pt(111) at the open-circuit potential (OCP) of 0.9 V. The resultant CV profile, shown as a dotted line in the inset of Figure 1, is essentially featureless. Meanwhile, this result resembles that of an iodine-modified Pt(111) electrode, revealed by the solid trace in the inset of Figure 1. This similarity in the CV characteristics implies that oxidation of iodobenzene molecules already occurred at the OCP upon their contact with the Pt(111) electrode. The level of charging current is sensitive to the surface roughness and adsorbed species.

To draw more comparisons between iodobenzene molecules and iodine atoms on Pt(111), we dosed the electrode with iodobenzene molecules at 0.4 V and swept the potential negatively to 0 V at 50 mV/s. A weak reduction feature emerging at 0.08 V gradually grew with continuous potential sweeping. The solid trace of Figure 2 shows the 12th scan. We associate this CV result with the coupled reactions of desorption of IB molecules and reduction of protons. The former process certainly gains importance at more negative potentials so that holding the potential at 0 V for 10 min could completely desorb the adsorbates. This view is well illustrated by the CV trace (dotted line in Figure 2), obtained after the stripping event. It is essentially identical to that of a well-ordered Pt(111) electrode. However, the products of this reductive desorption event were not identified. In contrast, if the same procedure was applied to a Pt(111) electrode coated with a monolayer of iodine atoms, potential holding at 0 V for 10 min or longer did not change the morphology of the CV traces. The solid and dotted traces in the inset of Figure 2 were acquired before and after the potential holding. These results tentatively reflect the relative strength of the interaction between the adsorbate of iodobenzene molecules and iodine atoms and the Pt(111) substrate. Iodine atoms are more strongly adsorbed than iodobenzene, inhibiting the adsorption of hydrogen even in 0.1 M $HClO_4$.

These CV results strongly suggest that iodobenzene could be molecularly adsorbed on a "wet" Pt(111) surface at room temperature. This view seemingly contradicts the UHV results, which show decomposition of IB molecules on all transition-metal surfaces of Pt, Au, Cu, Ag, and Pd at a temperature as low as 200 K.[21−25] However, as previously found for carbon monoxide,[27] molecular adsorption and the subsequent reactions may vary with the interfacial environments. In particular, the electrochemical potential, which controls the charge density at electrode surfaces, can influence the surface bonding. While the bonding of iodine on Pt electrodes is believed to be largely covalent, that of iodo molecules is unknown. Nevertheless, an aryl group apparently decreases the strength of surface bonding of the iodine headgroup on Pt. We also examined the adsorption of alkyl iodides, for example, iodoheptane and iodododecane, on Pt(111). The CV shown in inset a of Figure 2 is due to Pt-(111) coated with a monolayer of iodoheptane. Although inhibiting the adsorption of hydrogen between 0.3 and 0.05 V, the iodoheptane adlayer was completely desorbed by holding the potential at 0 V for 10 min. The CV feature at 0.65 V in the positive-going scan can result from a disorder−order phase transition, as observed with STM. Our STM results further suggest that iodoheptane molecules are more weakly adsorbed than iodobenzene.

We next consider the possibility of partial dissociation of iodo molecules and describe the method used to evaluate the coverage of iodobenzene. The process involves integrating the amount of charges contained in the stripping voltammograms in pH 10 $KClO_4$ solutions (Figure 3). The alkaline medium was used because molecular desorption and hydrogen evolution reactions otherwise overlap substantially in acidic solutions. We first ensure the adsorption of a full monolayer of iodobenzene molecules at 0.6 V, followed by initiating a negative-going potential sweep from 0.6 to 0 V at 50 mV/s. A pronounced reductive feature peaking at 0.08 V is attributable to the coupled reactions of one-electron reductive desorption of iodobenzene and proton reduction. The CV characteristics typical of an electrochemically clean Pt(111) immediately returned in the following positive-going sweep, indicating a complete desorption of the IB adlayer in a single negative-going sweep. The amount of charge, after correction for the double-layer charging, was about 110 $\mu C/cm^2$, which indicates a 0.45 coverage (number of IB molecules per Pt atom) if a one-electron reduction event is assumed. This value is in fact rather close to that (0.43) determined from the STM results to be described below. This stripping analysis has also been used to study alkanethiol molecules at Au(111) electrodes, usually resulting in correct coverages.[28,29]

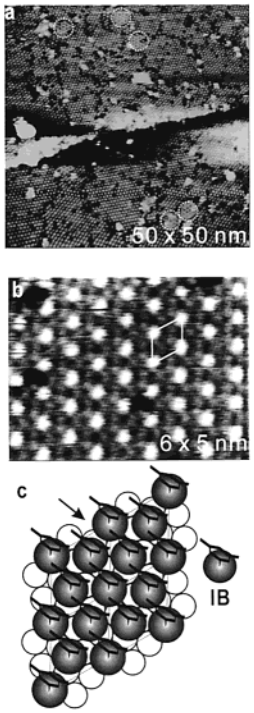

Figure 4. Constant-current in situ STM images of iodobenzene molecules chemisorbed on Pt(111) at 0.3 V. The bias voltage and set-point current are −150 mV and 6 nA, respectively. The model in (c) depicts the spatial structure seen in (b). The arrow points to the orientation of the molecular planes of the iodobenzene molecules.

Similarly, we applied this method to examine the coverage of iodine atoms on Pt(111), prepared by dosing with I_2 vapor after annealing. It was found that even a pH 10 $KClO_4$ solution was not enough to desorb iodine atoms so the experiments were done in pH 13 KOH solutions. The inset of Figure 3 presents the resultant CV profiles with the solid and dotted traces representing the first negative-going scan from 0.9 to 0 V and the immediate following sweep, respectively. The broad features ranging from 0.9 to 0.5 V are associated with the reductive desorption of iodine atoms to iodide ions. The charges of the corresponding reductive features for iodobenzene and iodine are roughly identical, which suggests a 0.45 coverage of the iodine atoms, assuming a one-electron reduction process. (The nonfaradaic charges were already accounted for in the process.) Reversing the scanning direction at 0 V results in the dotted line in the inset, and this cyclic voltammogram equals that of a well-defined Pt(111) electrode, implying a complete desorption of iodine atoms within a single potential scan.

In Situ STM Imaging of Iodobenzene Molecules. We first used STM to ensure acceptable surface cleanliness of a bare Pt(111) electrode, prepared by the annealing and quenching process. With its potential held at 0.3 V (within the double-layer charging region) in 0.1 M $HClO_4$, we then added the dosing solutions containing saturated iodoheptane (IH) or IB molecules. Real-time STM imaging revealed instantaneous, irreversible adsorption of a monolayer of IH or IB, forming two rather different molecular adlayers.

Figure 4 presents the constant-current STM images of iodobenzene on Pt(111) with its potential held at 0.3 V. The imaging parameters are −0.15 V and 6 nA. Figure 4a reveals a long-range ordered adlattice, presumably associated with the adsorption of iodobenzene molecules. The patchy appearance of the terrace arises from the presence of two rotational domains of an ordered structure, determined to be $(\sqrt{7} \times \sqrt{7})R19.1°$ from the high-resolution STM image in Figure 4b. In addition, the dotted circles in Figure 4b highlight another ordered array, identified as (3×3). Although both structures were previously observed for iodine atoms on Pt(111),[20] it is believed that these ordered structures are indeed due to iodobenzene molecules. At this point, we recall our aforementioned CV results, which clearly illustrate the fundamentally different electrochemical behavior between the Pt(111) electrodes modified with iodine atoms and iodobenzene molecules. These results lent strong support to the occurrence of molecular adsorption. This view would be further strengthened by the potential-dependent STM results. It is also worthwhile mentioning that the extent of ordering of iodobenzene also contrasts markedly with that of iodine atoms. While the former tends to form two rotational domains on a terrace, the latter usually forms a single ordered domain to reduce strains within the adlattice. The density of vacancy defects is usually rare for iodine adatoms, especially when prepared by gaseous dosing. The presence of many vacancy defects in Figure 4a further suggests that the adsorption process of iodobenzene could proceed with the nucleation-and-growth mechanism, leading to vacancy defects at the domain boundaries.

Figure 4b highlights the internal structure of the $(\sqrt{7} \times \sqrt{7})$-$R19.1°$ adlattice. The rhombus outlines the unit cell with an edge length of 0.74 nm. The clear corrugation pattern represents one of the most prominent features of this structure. The protrusions located at the four corners of the unit cell appear to be 0.05 nm higher than the weaker features. The latter are not as well resolved as those observed for iodine atoms.[20] However, the weaker features are considered genuine; otherwise, the internal of the cell would appear much darker than those defects in Figure 4b. This contention would imply a coverage of 0.43, identical to that of Pt(111)−$(\sqrt{7} \times \sqrt{7})R19.1°$−iodine atoms.[18,20] We present a tentative ball model in Figure 4c to show the molecular arrangement with the iodine heads coordinating to the Pt(111) surface as the iodine atoms do, i.e., one on top, one fcc, and one hcp per unit cell. Evidently, the orientations of all IB molecules have to align in a certain manner to minimize the intermolecular interaction. For example, we propose that the IB molecules all adapt stand-up configurations with their aromatic rings aligning parallel to the marked direction. This arrangement is likely to be rigid, leaving little free space for IB molecules to move. This rigidity can be helpful for achieving high-resolution STM images. We also note that the vacancy defects appearing in Figure 4b are all located at the 3-fold hollow sites, although they are thought to be the most favorable coordination sites. The corrugation height between the brightest features and the defects is averaged to be 0.25 nm.

Although the arrangements of iodine atoms and iodobenzene molecules are identical in the present situation, it is clear that this is not universally true. We compare, for example, sulfur and benzenethiol on Pt(111) and Au(111). Our preliminary results show that these two arrange similarly in $(\sqrt{3} \times \sqrt{3})$-$R30°$ on Pt(111). On the other hand, benzenethiol is adsorbed with a $(\sqrt{13} \times \sqrt{13})R13.9°$ symmetry on Au(111),[30] but sulfur forms $(\sqrt{3} \times \sqrt{3})R30°$.[31] These results suggest that the organic portions of the molecules can modify the interaction between the headgroups such as iodine or sulfur with the metal surfaces but the extent of their effects varies with the substrates.

STM Imaging of Iodoheptane. Figure 5 presents the constant-current STM images obtained on Pt(111) at 0.7 V in 0.1 M $HClO_4$ saturated with iodoheptane molecules. The STM imaging parameters are −50 mV and 2 nA. In contrast to the results of iodobenzene, which readily arranged in a well-ordered

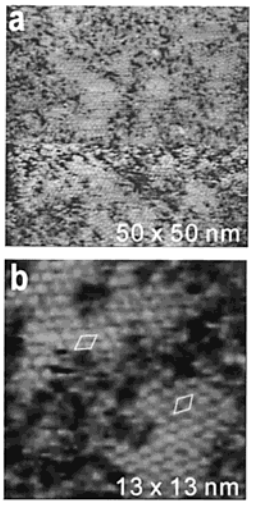

Figure 5. Constant-current in situ STM images of iodoheptane molecules chemisorbed on Pt(111) at 0.7 V. The bias voltage and feedback current are −50 mV and 2 nA, respectively.

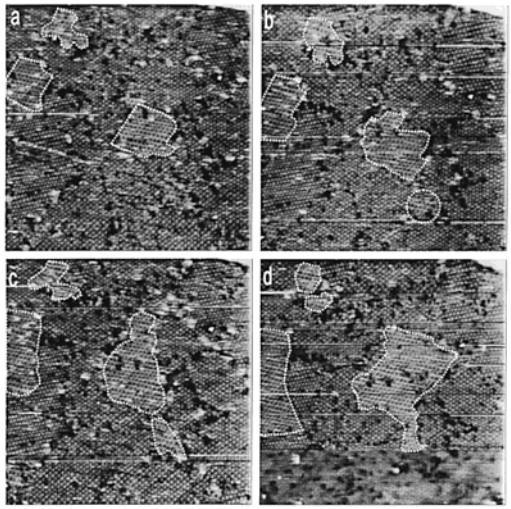

Figure 6. Time-dependent STM images of iodobenzene molecules on Pt(111), showing the reconstruction from $(\sqrt{7} \times \sqrt{7})R19.1°$ to (3×3), as the potential was stepped from 0.3 to 0.55 V. The time differences for these images were all 16 s. The tunneling parameters are −50 mV and 2 nA. (Scan size 40 × 40 nm.)

$(\sqrt{7} \times \sqrt{7})R19.1°$ array at most potentials, iodoheptane was mostly disordered at potentials negative of 0.7 V. Only making the potential more positive could render local organization, but the degree of ordering was never as good as that of iodobenzene. For example, the sizes of the ordered arrays rarely exceed 10 nm, much less than hundreds of nanometers found for iodobenzene. This strong dependence of molecular arrangements on the potential manifests itself on the CV profile (inset a in Figure 2), where a weak feature at 0.65 V emerges. Tentatively, this phenomenon originates from a potential-induced increase of coverage of iodoheptane, similarly reported for iodine atoms.[32]

Meanwhile, the tip-and-sample interaction becomes more pronounced for iodoheptane, because the tip readily wipes out local ordered structures. A faction of the STM image in Figure 5a reveals this effect. This phenomenon is certainly not observed for iodine atoms, which can give images with unusual parameters of 50 nA and 5 mV.[33] Again, it is believed that these ordered arrays are entirely due to iodoheptane molecules, rather than iodine atoms. Figure 5b presents the high-resolution STM image of the ordered array, also characterized as $(\sqrt{7} \times \sqrt{7})R19.1°$ with the two rhombuses representing its two rotational domains. Although it is not immediately clear in this image, its coverage and packing are essentially equivalent to those of iodobenzene. The average corrugation height, measured to be 0.30 nm, is about 0.05 nm higher than that of iodobenzene.

Imaging Contrast of Iodobenzene and Iodoheptane Monolayers. The fact that we could employ rather low tunneling resistances (1−10 MΩ) to obtain stable molecular resolution of iodobenzene indicates that the tip was traveling above the molecular plane with an acceptable tip-and-sample interaction. Notably, these values are 3 orders of magnitude smaller than those used in UHV STM for imaging alkanethiol on Au(111), a seemingly surprising result. On the other hand, if one refers to the reported STM results of all molecular adsorbates in ambient conditions or in solutions, the tunneling resistances are all in the neighborhood of 10 MΩ. One of the possible reasons for the difference is that the tunneling barrier for STM imaging varies substantially with the environments. For example, Nagatani et al. employed Pt and W tips to measure tunneling barriers of bare Au, Pt, and iodine-modified Au and Pt electrodes in electrolytes and UHV.[34] In any case, the adsorption of iodine atoms substantially reduced the tunneling barriers. The value can be as low as 0.35 eV for the I/Au(111) system. We have found two prominent effects to be responsible for these results. First, the conducting media of aqueous electrolytes contribute greatly to this effect. Second, iodine adsorbates donate charges to substrates and thereby largely reduce the work functions of the electrodes.[35]

Next, we consider how the aliphatic and aromatic hydrocarbons affect the charge donation from the iodine headgroup to the Pt substrate. The long alkane chains are generally believed to be insulating because their LUMO and HOMO levels differ by 9 eV.[13] They should not contribute to the tunneling event, as indeed observed in UHV. On the other hand, they might influence the charge distribution of iodobenzene and iodoheptane molecules at the electrified interfaces. In particular, the phenyl group is considered to be more electron donating than an alkyl group, so the former could induce more charge transfer. According to the classical tunneling theory models, an exponential relationship between tunneling current and tunneling barrier,[36] this would result in lowering of the work function and tunneling barrier. Local sites with a lower tunneling barrier are expected to give higher corrugation when images are taken under identical tunneling resistances. To unravel this effect, we compare the corrugation heights of the molecular images of iodobenzene, iodoheptane, and iodine atoms with respect to a near vacancy defect, such as those seen in Figures 4b and 5b. The values are 0.2, 0.3, and 0.16 nm, respectively. The higher corrugation for iodobenzene, as compared to that of iodine atoms, can imply an enhancement of charge transfer by the phenyl group. However, it is not clear why iodoheptane results in an even higher corrugation than that of iodobenzene. We recall that the iodoheptane adlayer appears to be much less stable in the STM imaging, likely due to the stronger tip-and-sample interaction. In this case, the tip might have an anomalous effect on the density of states of an iodoheptane-coated Pt(111) surface. A similar effect was previously noted for octanethiol adsorbed on Au(111), where molecular conformations render different corrugations.[10−13]

Potential-Induced Rearrangement of Iodobenzene Molecules on Pt(111). Here, we present potential-dependent STM imaging of iodobenzene molecules, emphasizing the different consequences of the modulation of potential on the structures of the adlayers, as compared to iodine atoms. Figure 6 reveals the time-dependent STM images obtained for iodobenzene

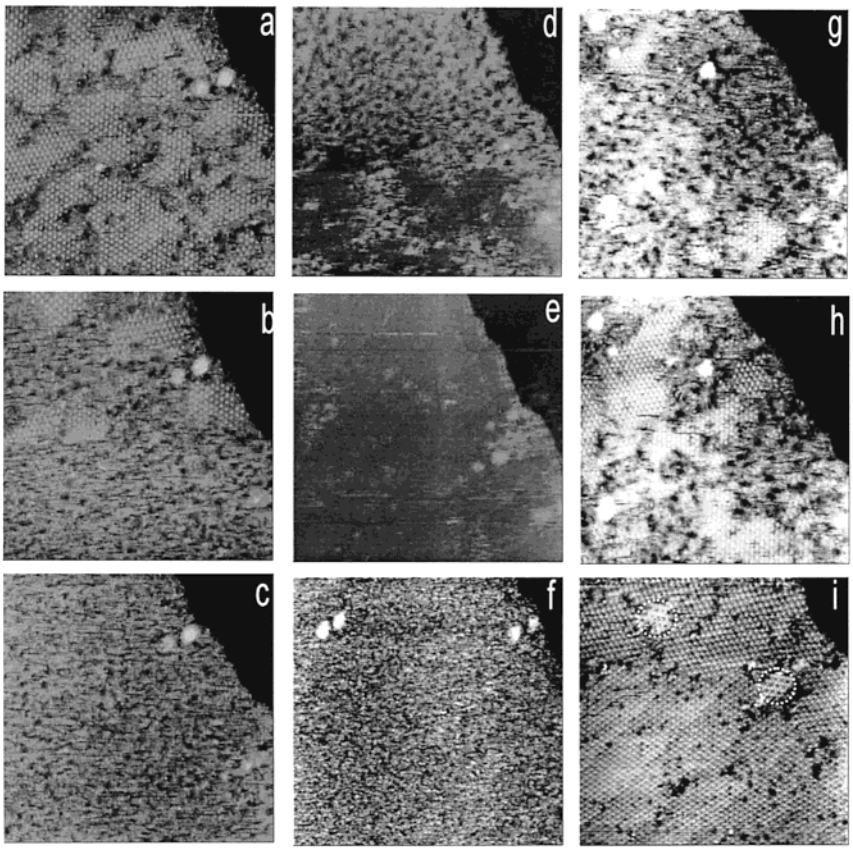

Figure 7. Time-dependent in situ STM images, showing the reversible desorption and adsorption of iodobenzene molecules on Pt(111). The potentials for these images were 0.2 V (a), 0.1 V (b), 0.1 V (c), 0.05 V (d and e), 0.1 V (f), 0.2 V (g), 0.2 V (h), and 0.4 V (i). (Scan size 35 × 35 nm.)

molecules after the potential of Pt(111) was stepped from 0.3 to 0.55 V in a 0.1 M $HClO_4$ solution containing saturated iodobenzene. The differences in time for these STM images are 16 s. First, one notes the presence of a few local (3 × 3) domains amid a main structure of ($\sqrt{7} \times \sqrt{7}$)*R*19.1° in Figure 6a, but the abrupt change of potential readily rearranges ($\sqrt{7} \times \sqrt{7}$)*R*19.1° to (3 × 3). The coverages of ($\sqrt{7} \times \sqrt{7}$)*R*19.1° and (3 × 3) are 0.43 and 0.44, respectively.[18,20] The (3 × 3) domains are highlighted by the dotted outlines. This rearrangement event occurred preferentially at the locations where (3 × 3) structures are originally located and grew with time at the expense of the ($\sqrt{7} \times \sqrt{7}$)*R*19.1° structure. The appearance of the ($\sqrt{7} \times \sqrt{7}$)*R*19.1° structure resembles the asymmetric, rather than the symmetric, (3 × 3) pattern. This phase transition was reversible to the modulation of potential. In contrast, STM reveals that iodine atoms on Pt(111) are exceedingly slow to change with potential at room temperature,[37] although UHV results show reconstruction from ($\sqrt{7} \times \sqrt{7}$)*R*19.1° to (3 × 3) at potentials positive of 0.6 V.[18] These differences should reflect the relative strength of surface bonding involving iodine or iodo molecules with the Pt substrate. A stronger binding force for iodine atoms renders higher resistances toward potential changes. This view seems to hold also for the changes brought about by the imposition of more negative potentials.

Shown in Figure 7 are potential- and time-dependent STM images, obtained by gradually stepping the potential from 0.2 to 0.05 V (a−e), and then sequentially back from 0.05 to 0.4 V (f−i). A pair of extrabright features and the neighboring step ledge at the upper right corner act as the markers to guide against the thermal drift encountered during the STM imaging. In line with the CV results in Figure 2, stepping the potential from 0.2 to 0.1 V brought about instantaneous changes, as the originally ordered ($\sqrt{7} \times \sqrt{7}$)*R*19.1° domains shrunk markedly 64 s later (b) and disappeared to bring up an entirely roughened adlayer 47 s later (c). It therefore appears that the phase transitions were initiated at the domain boundaries, and continued to creep preferentially along the perimeter of ordered domains.

These STM results unambiguously illustrate that negative potential polarization could decrease the coverage and even remove the entire monolayer of iodobenzene molecules. In contrast, as indicated by the CV results in Figure 1, these events would not be possible for iodine adatoms. Even though the ordered ($\sqrt{7} \times \sqrt{7}$)*R*19.1° pattern seems to disappear, iodobenzene still predominately covered the surface even at 0.1 V, the onset of hydrogen evolution. The increase of molecular motion can be responsible for the lack of ordering under this circumstance. The adsorption of hydrogen was still minor at 0.1 V, but finally gained importance at 0.05 V, as shown in Figure 7d. The hydrophobic nature of these organic species rendered segregation from the hydrophilic domains of hydrogen atoms. Replacement of IB molecules with hydrogen atoms continued to remove all the IB molecules 38 s later, resulting in a "uniform" Pt(111) surface (Figure 7e). Thus, desorption of IB molecules in aqueous solutions is preceded by a disordering event, where the hydrophobic interaction among the organic alkyl chains could prevent the IB molecules from directly dissolving. An apparently related two-step process was previously noted for the desorption of alkanethiol molecules from Au(111).[29]

To show the reversibility of the desorption/adsorption events, we first stepped the potential from 0.05 V back to 0.1 V. The STM image immediately turned "fuzzy", suggesting the occurrence of adsorption of foreign species (Figure 7f). As the potential was stepped to 0.2 V, some locally ordered structures, iden-

tified as ($\sqrt{7} \times \sqrt{7}$)*R*19.1°, emerged (Figure 7g). This ($\sqrt{7} \times \sqrt{7}$)*R*19.1° adlattice seemingly has to arise from the adsorption of iodobenzene, and grew rapidly as the potential was stepped in the positive direction to 0.4 V. Meanwhile, some occasional (3×3) patches, as noted by the dotted circle in Figure 7i, appear amid a predominate ($\sqrt{7} \times \sqrt{7}$)*R*19.1° structure.

Finally, we briefly compare our present CV and STM results with those obtained for the adsorption of iodobenzene at Pt(111) in UHV. High-resolution electron energy loss spectroscopy (HREELS) has been one of the most useful tools in probing the molecular vibrations of organic adsorbates. For example, Cabibil et al. employed HREELS to show that iodobenzene molecules lie flat at a Pt(111) surface, interacting with the substrate with both the iodine end and the aromatic portion of the molecules.[23] This molecular configuration is apparently different from our present results. One of the possible causes for this discrepancy could be the different dosage levels of iodobenzene molecules in these two environments. With the concentrations of these organic iodo molecules in the neighborhood of mM, nearly 2000 times higher than those used in UHV, they could adopt upright configurations to accommodate more adsorbates.[10−13] As a corollary, molecules may lie down to align parallel to the surfaces when their concentrations become low. In fact, in situ STM imaging performed in diluted iodobenzene solutions revealed an entirely different real-space structure. We are currently investigating this structure.

Conclusion

The electrode potential is crucial to the chemical nature of iodobenzene and iodoheptane molecules adsorbed on a well-ordered Pt(111). At potentials negative of 0.9 V, these molecules are adsorbed intact with their iodo ends binding with the Pt substrate. Degradation only occurred at more positive potentials. The strength of surface bonding appears to follow the order iodine > iodobenzene > iodoheptane. While iodobenzene arranges in well-ordered (3×3) and ($\sqrt{7} \times \sqrt{7}$)*R*19.1°, iodoheptane is largely disordered until the potential is made more positive than 0.7 V. Overall, a phenyl functional group exerts less influence on the surface bonding of the iodine headgroup on Pt than an aliphatic alkyl chain such as C7 or C12. The time- and potential-dependent high-quality STM imaging unambiguously illustrates the dominating role of the potential on the coverages of these molecules. These results contrast markedly with those of iodine atoms, whose coverages and structures vary little with the potential, indirectly indicating that the adsorbing species are indeed iodo molecules, rather than iodine atoms produced by decomposition.

The stability of STM imaging of iodobenzene indicates that the scanning probe was traveling atop the molecular adlayer, exerting minimal perturbation to the molecular adlayers, even though the tunneling resistances used in our experiments are 2−3 orders of magnitude lower than those of UHV-STM. The strong resemblance of iodobenzene to the iodine atoms in the STM images indicates that the scanning tunneling microscope was mainly imaging the iodine headgroups attaching to the Pt(111) substrate, while the phenyl and alkyl portions of the molecules are invisible. Finally, the tip interacts more strongly with the alkyl chains of iodoheptane, rendering frequent changes of its spatial arrangements in the course of imaging.

Acknowledgment. This work is supported by the National Science Council of the Republic of China under Contract No. NSC 90-2119-M-008-002. We are grateful to Dr. L. J. Fan and Dr. W. Y. Yang at the SRRC of Taiwan for their help. We thank Prof. M. J. Weaver for proofreading this manuscript carefully. Financial support from the Helix Cooperation is greatly appreciated.

References and Notes

(1) Binning, G.; Rohrer, H.; Gerber, Ch.; Weibel, E. *Phys. Rev. Lett.* **1983**, *50*, 120.
(2) Itaya, K. *Prog. Surf. Sci.* **1998**, *58*, 121.
(3) Sautet, P. *Surf. Sci.* **1997**, *374*, 406.
(4) Tilinin, I. S.; Rose, M. K.; Dunphy, J. C.; Salmeron, M.; Van Hove, M. A. *Surf. Sci.* **1998**, *418*, 511.
(5) Sautet, P.; Bocquet, M.-L. *Phys. Rev. B* **1996**, *53*, 4910.
(6) Yau, S.-L.; Kim, Y.-G.; Itaya, K. *J. Am. Chem. Soc.* **1996**, *118*, 7795.
(7) Lee, H. S.; Iyengar, S.; Musselman, I. H. *Anal. Chem.* **2001**, *73*, 5532.
(8) Ohshiro, T.; Ito, T.; Buhlmann, P.; Umezawa, Y. *Anal. Chem.* **2001**, *73*, 878.
(9) Ulman, A. *Chem. Rev.* **1996**, *96*, 1533.
(10) Poirier, G. E. *Chem. Rev.* **1997**, *97*, 1117.
(11) Poirier, G. E.; Pylant, E. D. *Science* **1996**, *272*, 1145.
(12) Schönenberger, C.; Jorritsma, J.; Sondag-Huethorst, J. A. M.; Fokkink, L. G. J. *J. Phys. Chem.* **1995**, *99*, 3259.
(13) Takami, T.; Delamarche, E.; Michel, B.; Gerber, Ch.; Wolf, H.; Ringsdorf, H. *Langmuir* **1995**, *11*, 3876.
(14) Yang, J.-S.; Lee, C.-C.; Yau, S.-L,; Chang, C.-C.; Lee, C.-C.; Leu, J.-M. *J. Org. Chem.* **2000**, *65*, 871.
(15) Tao, Y. T.; Wu, C. C.; Eu, J. Y.; Lin, W. L. *Langmuir* **1997**, *13*, 4018.
(16) Hsieh, M.-H.;Chen, C.-H. *Langmuir* **2000**, *16*, 1729.
(17) Sawaguchi, T.; Sato, Y.; Mizutani, F. *J. Electroanal. Chem.* **2001**, *507*, 256.
(18) Hubbard, A. T. *Chem. Rev.* **1988**, *88*, 633.
(19) Yau, S.-L.; Vitus, C. M.; Schardt, B. C. *J. Am. Chem. Soc.* **1990**, *112*, 3677.
(20) Schardt, B. C.; Yau, S.-L.; Rinaldi, F. *Science* **1989**, *243*, 1050.
(21) Yang, M. X.; Xi, M.; Yuan, H.; Bent, B. E.; Stevens, P.; White, J. M. *Surf. Sci.* **1995**, *341*, 9.
(22) Syomin, D.; Koel, B. E. *Surf. Sci.* **2001**, *490*, 265.
(23) Cabibil, H.; Ihm, H.; White, J. M. *Surf. Sci.* **2000**, *447*, 91.
(24) Jaramillo, D. M.; Hunka, D. E.; Land, D. P. *Surf. Sci.* **2000**, *445*, 23.
(25) Szulczewski, G. J.; White, J. M. *Surf. Sci.* **1998**, *399*, 305.
(26) Clavilier, J.; Rodes, A.; El Achi K.; Zamakhchari, M. A. *J. Chim. Phys. Phys.-Chim. Biol.* **1991**, *88*, 1291.
(27) Villegas, I.; Weaver, M. J. *J. Chem. Phys.* **1994**, *101*, 1648.
(28) Tao, Y. T.; Wu, C. C.; Eu, J. Y.; Lin, W. L. *Langmuir* **1997**, *13*, 4018.
(29) Wang, S. S.; Porter, M. D. *J. Electroanal. Chem.* **2000**, *485*, 135.
(30) Wan, L. J.; Terashima, M.; Noda, H.; Osawa, M. *J. Phys. Chem. B* **2000**, *104*, 3563.
(31) Vericat, C.; Vela, M. E.; Andreasen, G.; Salvarezza, R. C.; Vazquez, L.; Martin-Gago, J. A. *Langmuir* **2001**, *17*, 4919.
(32) Lu, F.; Salaita, G. N.; Baltruschat, H.; Hubbard, A. T. *J. Electroanal. Chem.* **1987**, *222*, 305.
(33) Yau, S. L. Ph.D. Thesis, Purdue University, Lafayette, IN, 1990.
(34) Nagatani, Y.; Hayashi, T.; Yamada, T.; Itaya, K. *Jpn. J. Appl. Phys.* **1996**, *35*, 720.
(35) Jo, S. K.; White, J. M. *Surf. Sci.* **1992**, *261*, 111.
(36) Lang, N. D. *Phys. Rev. Lett.* **1985**, *55*, 230.
(37) Inukai, J.; Osawa, Y.; Wakisaka, M.; Sashikata, K.; Kim, Y.-G.; Itaya, K. *J. Phys. Chem.* **1998**, *102*, 3498.